

## Supporting Information

*of*

### **Tumor-Triggered Drug Release with Tumor-Targeted Accumulation and Elevated Drug Retention to Overcome Multidrug Resistance**

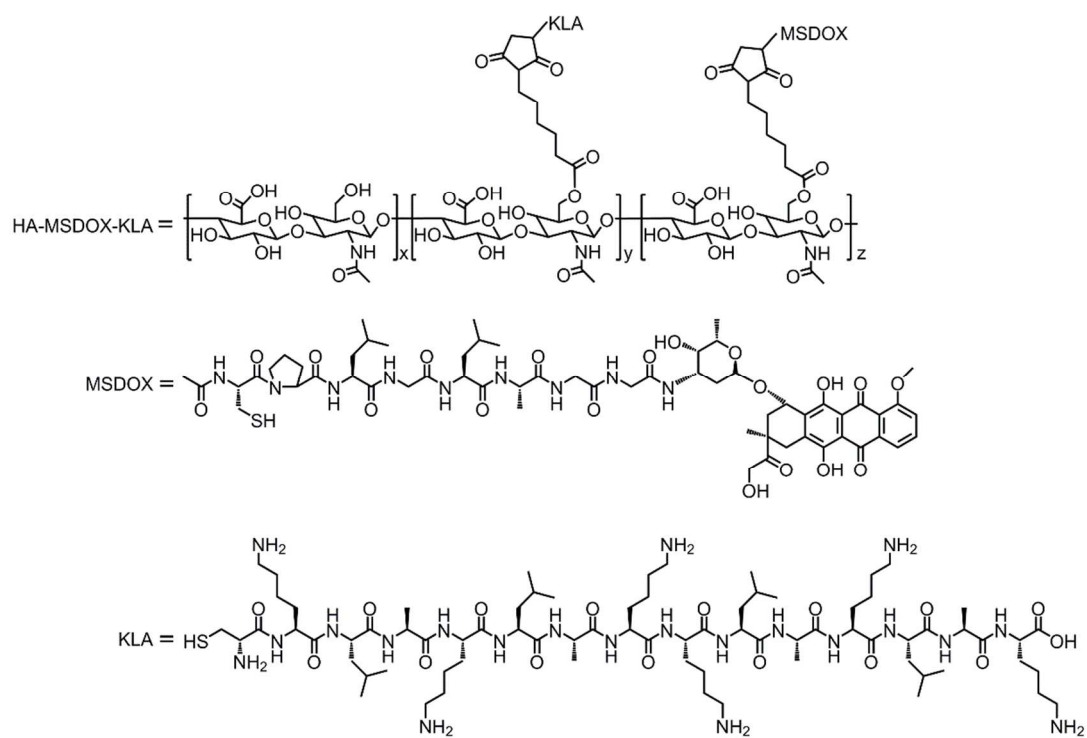
Wei-Hai Chen,<sup>1,†</sup> Guo-Feng Luo,<sup>1,†</sup> Wen-Xiu Qiu,<sup>1</sup> Qi Lei,<sup>1</sup> Li-Han Liu,<sup>1</sup> Di-Wei Zheng,<sup>1</sup> Sheng Hong,<sup>1</sup> Si-Xue Cheng,<sup>1</sup> and Xian-Zheng Zhang<sup>1,2\*</sup>

<sup>1</sup> Key Laboratory of Biomedical Polymers of Ministry of Education & Department of Chemistry,  
Wuhan University, Wuhan 430072, P. R. China

<sup>2</sup> The Institute for Advanced Studies, Wuhan University, Wuhan 430072, P. R. China

\*Corresponding Author: xz-zhang@whu.edu.cn

†These authors contributed equally to this work.



**Scheme S1.** The chemical structure of HA-MSDOX-KLA.

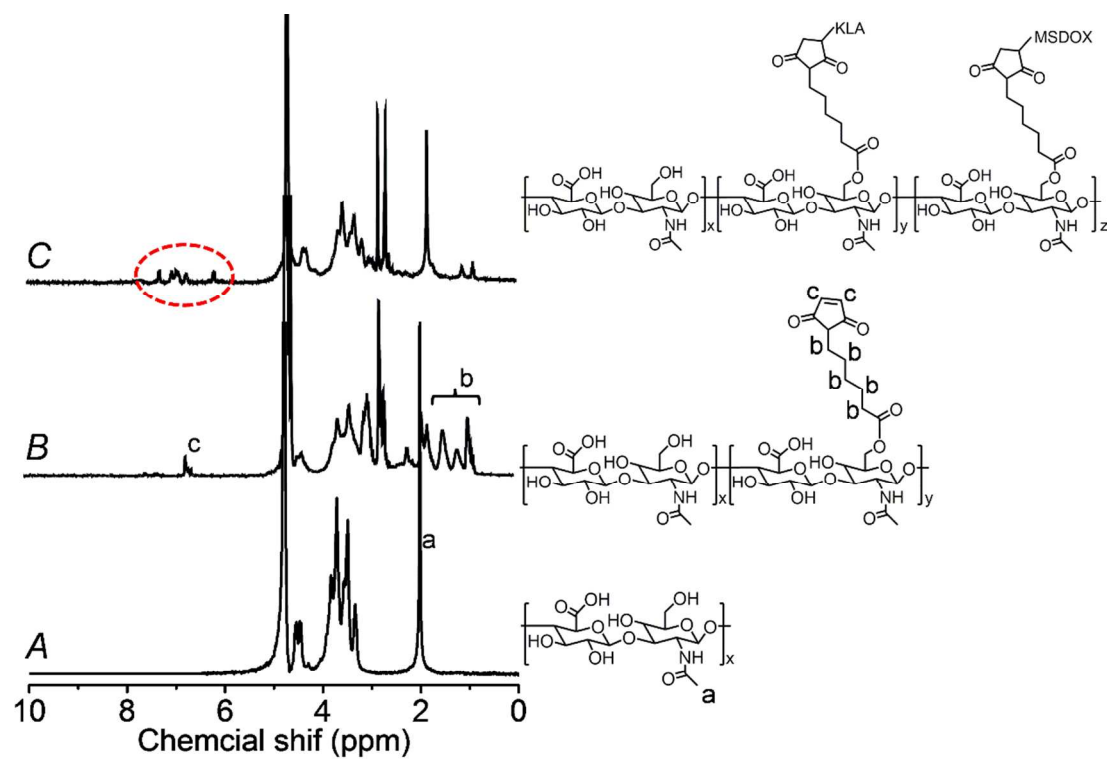


**Figure S1.**  $^1\text{H}$  NMR spectra of HA (A), HA-Mal (B), and HA-MSDOX-KLA (C). The red ellipse indicated the typical  $^1\text{H}$  NMR peaks of benzene rings, which belonged to the DOX in HA-MSDOX-KLA.

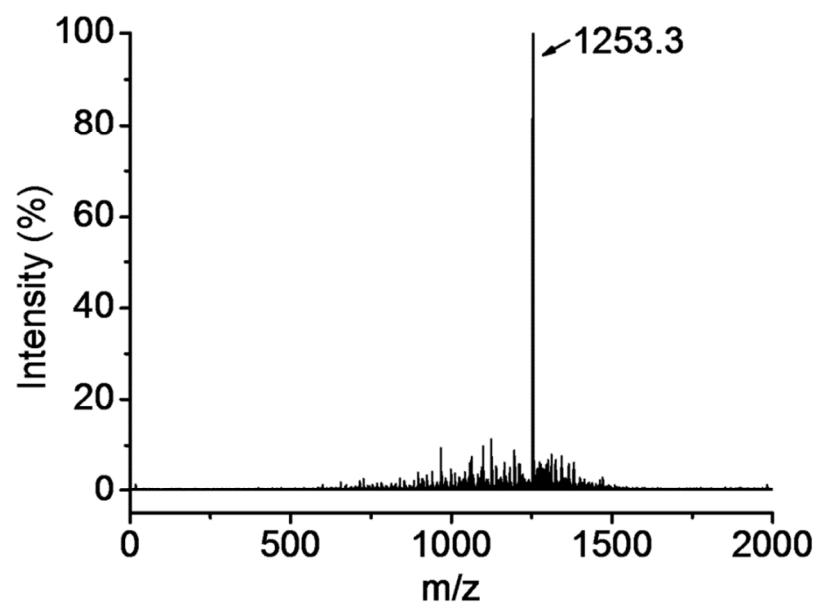


**Figure S2.** MALDI-TOF-MS of MSDOX.

ESI-2015-11-6-6-1 #1 RT: 0.02 AV: 1 NL: 8.23E8  
T: + c ESI Full ms [50.00-2000.00]

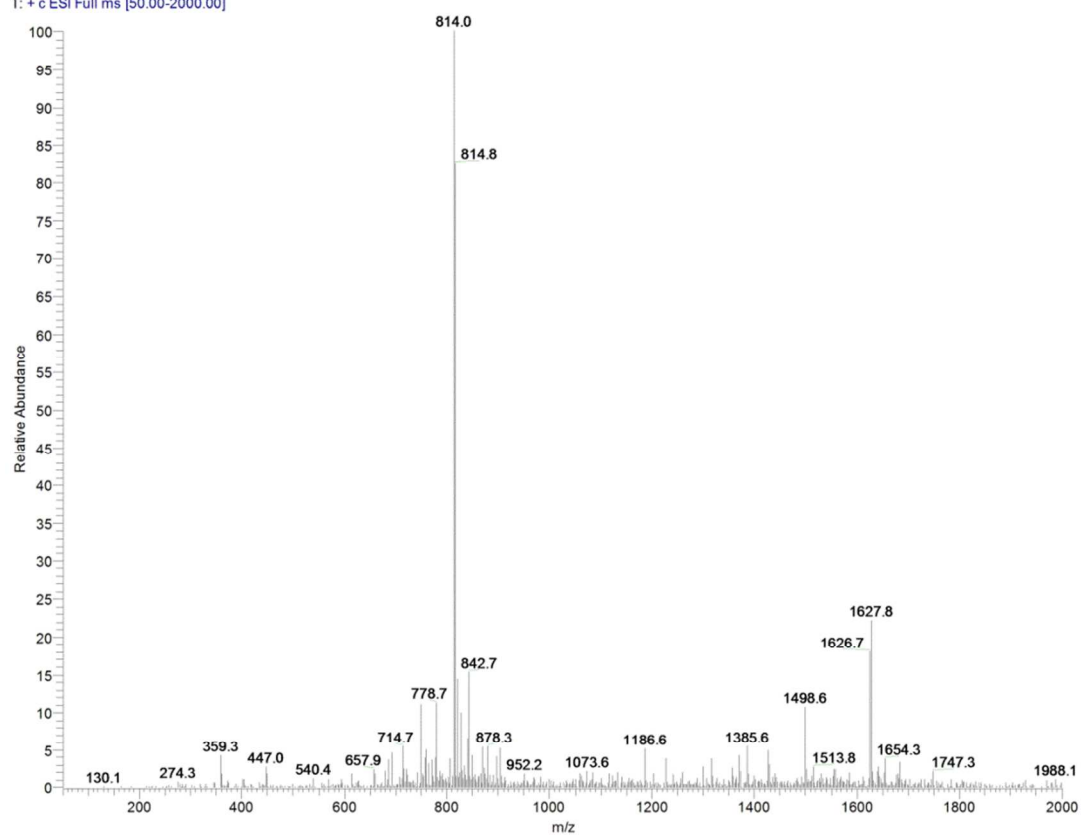


**Figure S3.** ESI-MS of KLA.

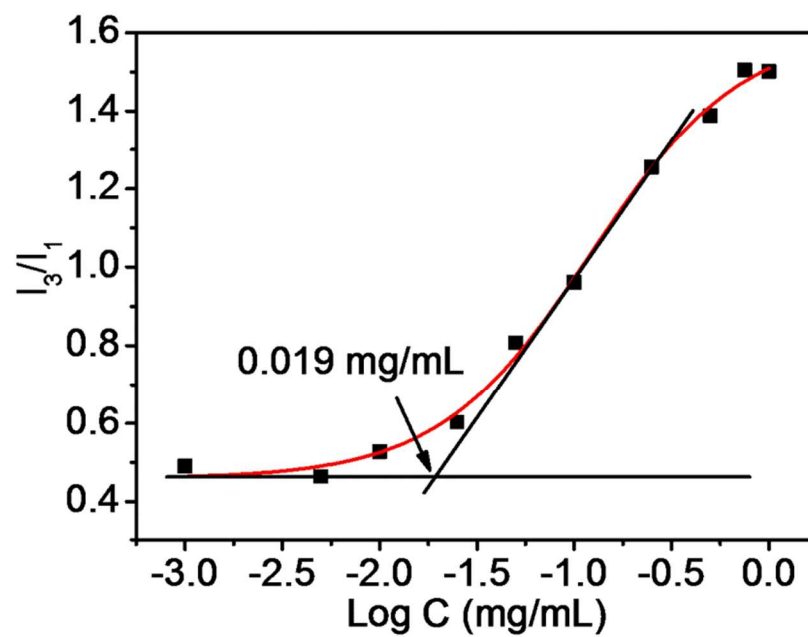


**Figure S4.** The CMC of HA-MSDOX-KLA micelles determined by fluorescence spectra and using pyrene as a hydrophobic fluorescent probe. Plot of the intensity ratio  $I_3/I_1$  vs log C, the measured CMC value was 0.019 mg/mL.

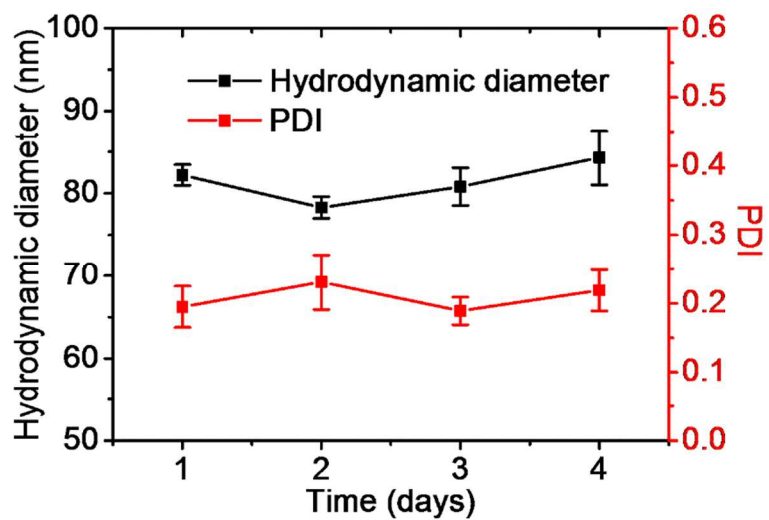


**Figure S5.** The hydrodynamic diameter and polydispersity index (PDI) of the HA-MSDOX-KLA micelles in PBS with 10% serum proteins (FBS) investigated for four days by DLS.

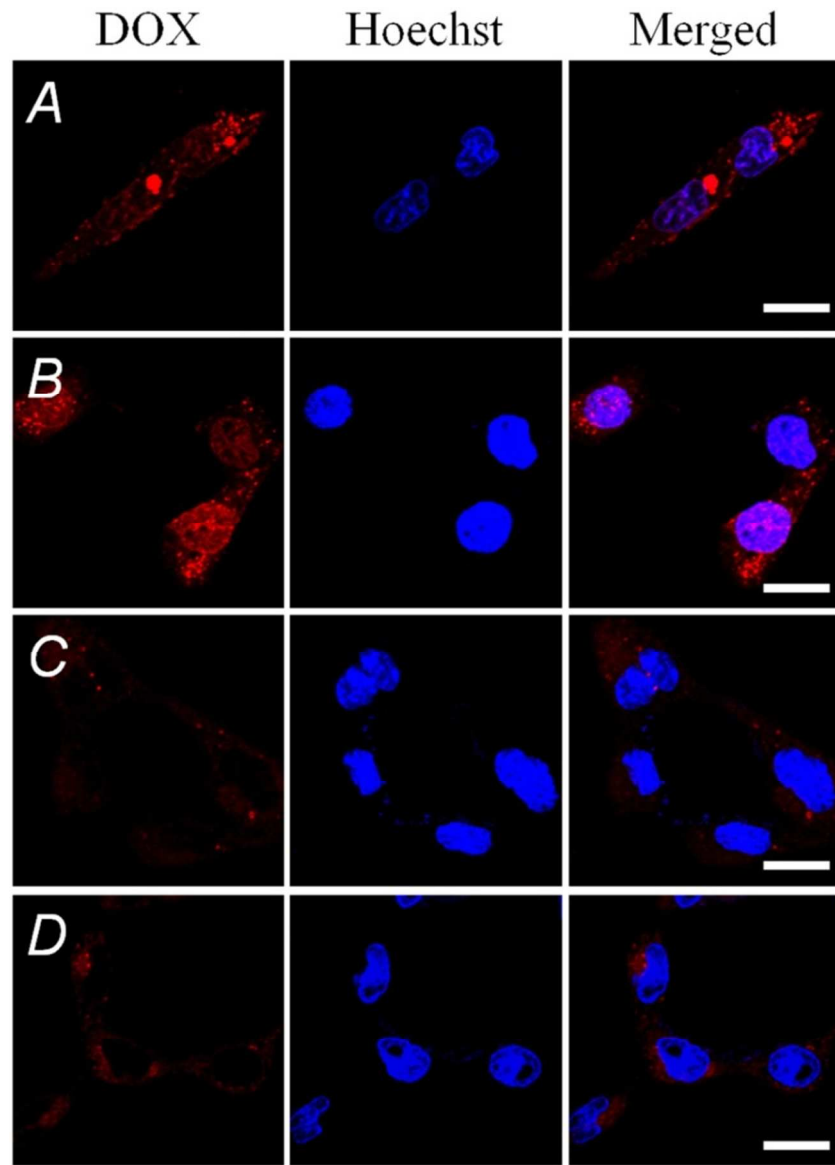


**Figure S6.** A) and B) Confocal laser scanning microscopy (CLSM) images of COS7 cells treated with free DOX for 6 h or 12 h, respectively. C) and D) CLSM images of COS7 cells treated with HA-MSDOX-KLA for 6 h or 12 h, respectively. The nuclei are stained by Hoechst 33342. Scale bar: 20  $\mu\text{m}$ .



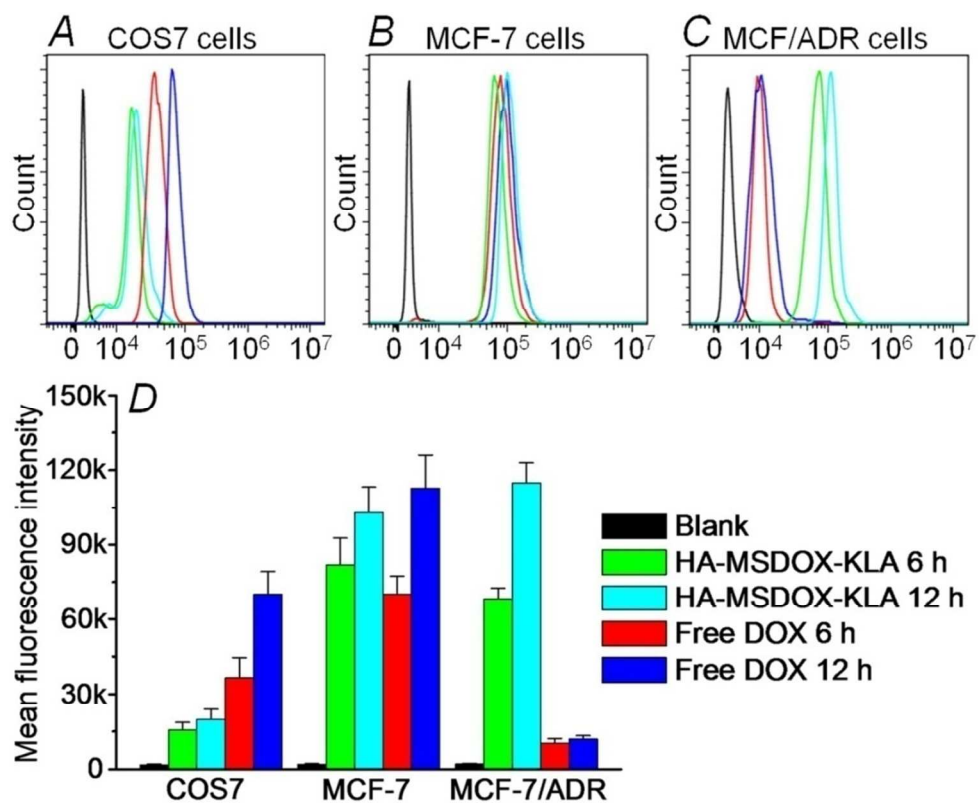


**Figure S7.** Flow cytometry analysis of intracellular uptake of DOX in COS7 cells (A), MCF-7 cells (B), and MCF/ADR-7 cells (C), respectively. D) The corresponding mean fluorescence intensity displayed in Figure S7A-7C. The cells treated with HA-MSDOX-KLA for 6 h (green) and 12 h (cyan), the cells treated with free DOX for 6 h (red) and 12 h (blue), and the cells without treatment were used as the control (black).

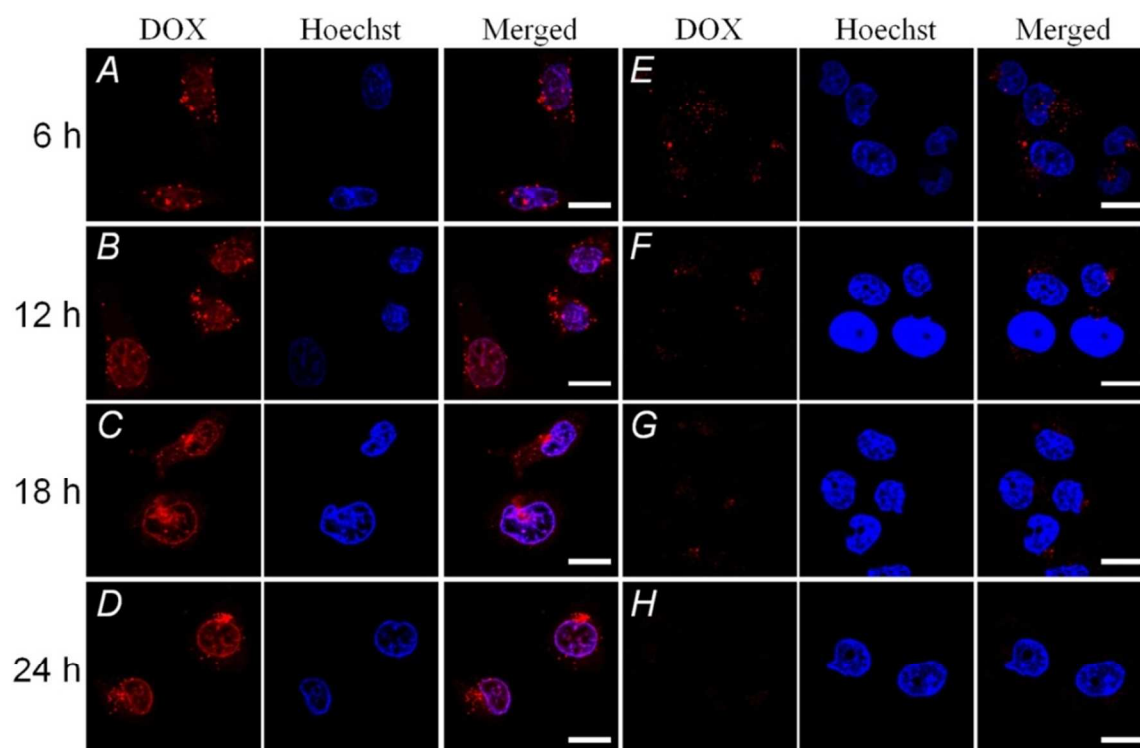


**Figure S8.** A-D) CLSM images of MCF-7 cells (the cells were pre-treated with free DOX for 6 h) for additional incubation with fresh culture medium of 6 h, 12 h, 18 h and 24 h, respectively. E-H) CLSM images of MCF-7/ADR cells (the cells were pre-treated with free DOX for 6 h) for additional incubation with fresh culture medium of 6 h, 12 h, 18 h and 24 h, respectively. The nuclei are stained by Hoechst 33342. Scale bar: 20  $\mu\text{m}$ .

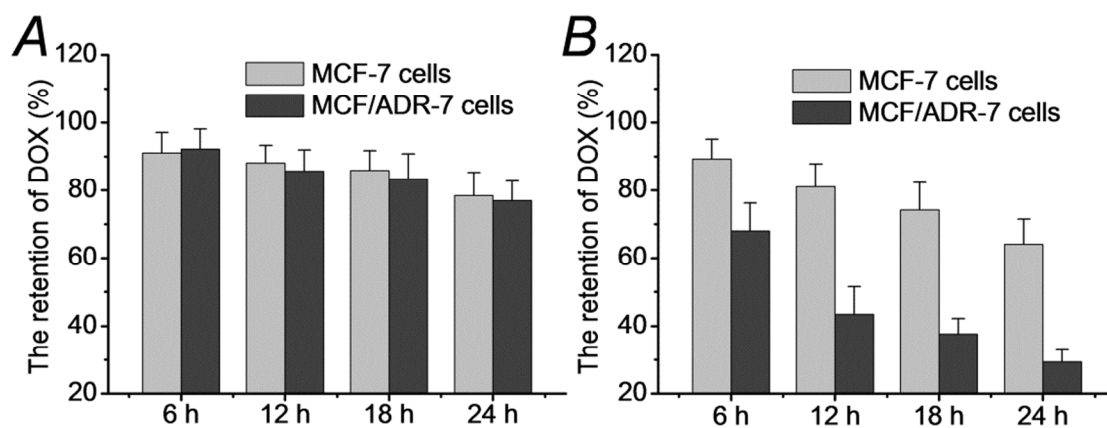


**Figure S9.** Statistical quantification of corresponding intracellular retention DOX via software Image-J. A) MCF-7 and MCF-7/ADR cells treated with HA-MSDOX-KLA. B) MCF-7 and MCF-7/ADR cells treated with free DOX.

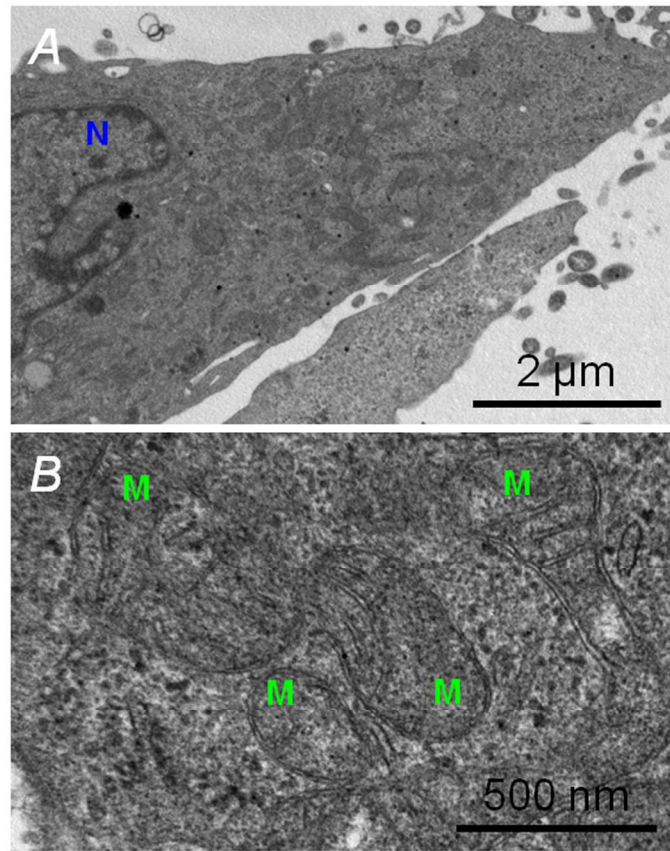


**Figure S10.** A) and B) Bio-TEM images of MCF-7/ADR cells without HA-MSDOX-KLA treatment. The blue “N” represents nuclei and the green “M” represents mitochondria.

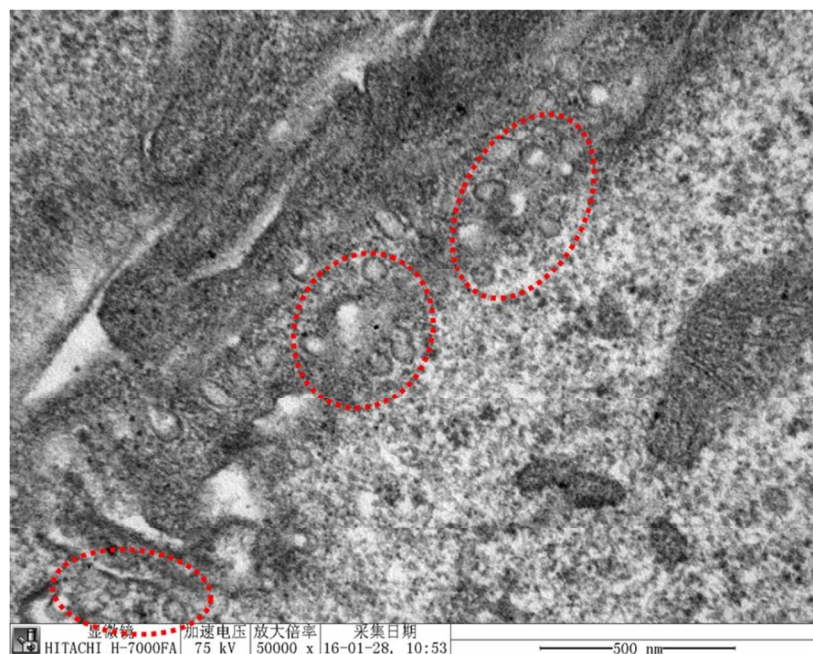


**Figure S11.** Bio-TEM images of MCF-7/ADR cells treated with HA-MSDOX-KLA for 6 h.

HA-MSDOX-KLA nanoparticles are highlighted by red circles.

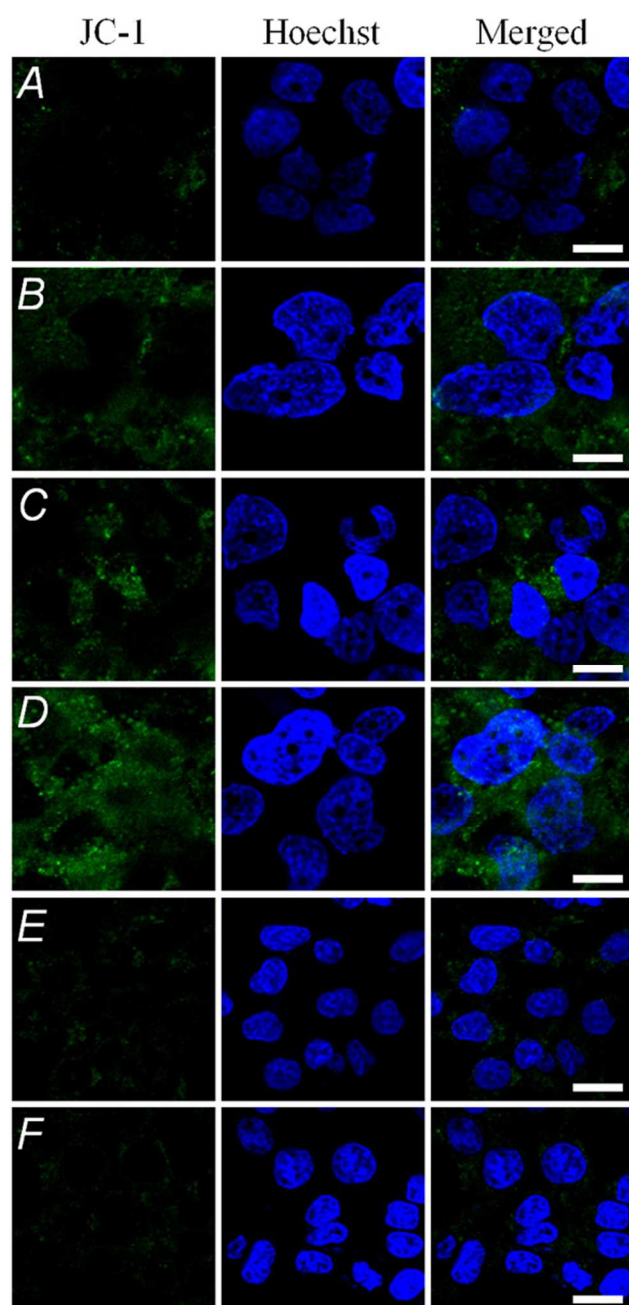


**Figure S12.** Analysis of mitochondrial membrane potential by JC-1 assay. A) MCF-7/ADR cells without any treatment. B-D) MCF-7/ADR cells treated with HA-MSDOX-KLA for 12 h, 24 h and 48 h, respectively. E) COS7 cells without any treatment. F) COS7 cells treated with HA-MSDOX-KLA for 48 h. The nuclei are stained by Hoechst 33342. Scale bar: 20  $\mu\text{m}$ . The increased green fluorescence (JC-1 monomer in the cytoplasm) can be observed in MCF-7/ADR cells incubated with HA-MSDOX-KLA (Figure S12B-S12D), indicating that the mitochondria of MCF-7/ADR cells are destroyed seriously, leading to a relatively low  $\Delta\Psi\text{m}$ .

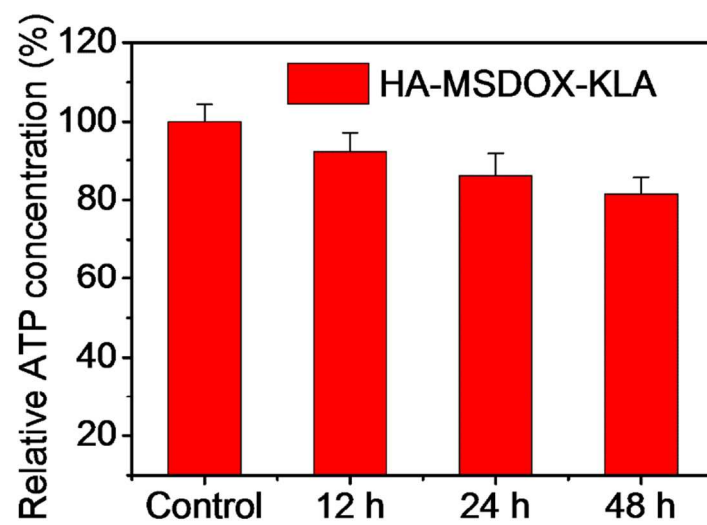


**Figure S13.** Relative ATP levels of COS7 cells after treatment with HA-MSDOX-KLA.

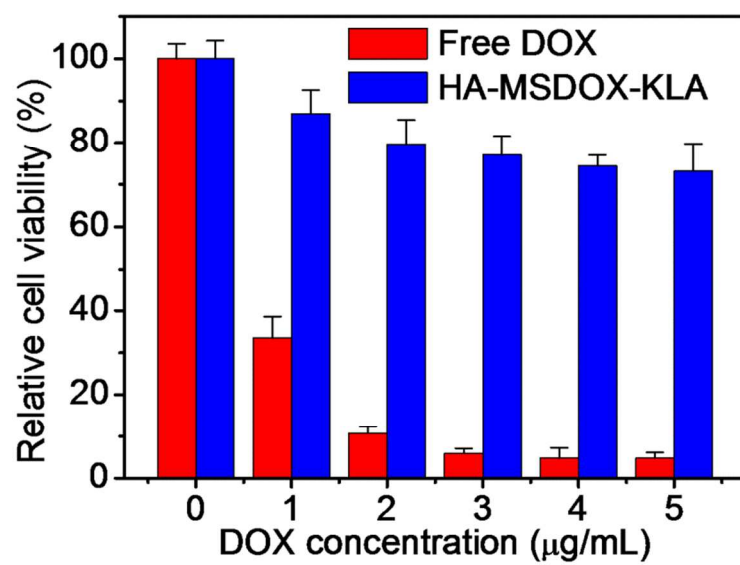


**Figure S14.** Cytotoxicity of free DOX and HA-MSDOX-KLA against COS7 cells.



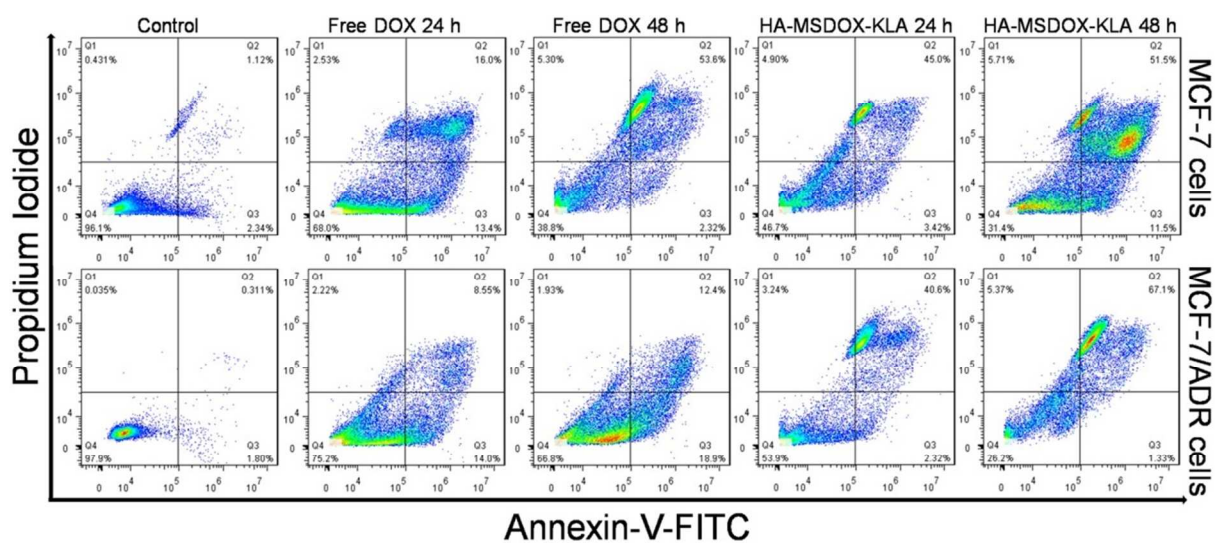


**Figure S15.** Evaluation of apoptosis in MCF-7 cells and MCF-7/ADR cells with different treatments.

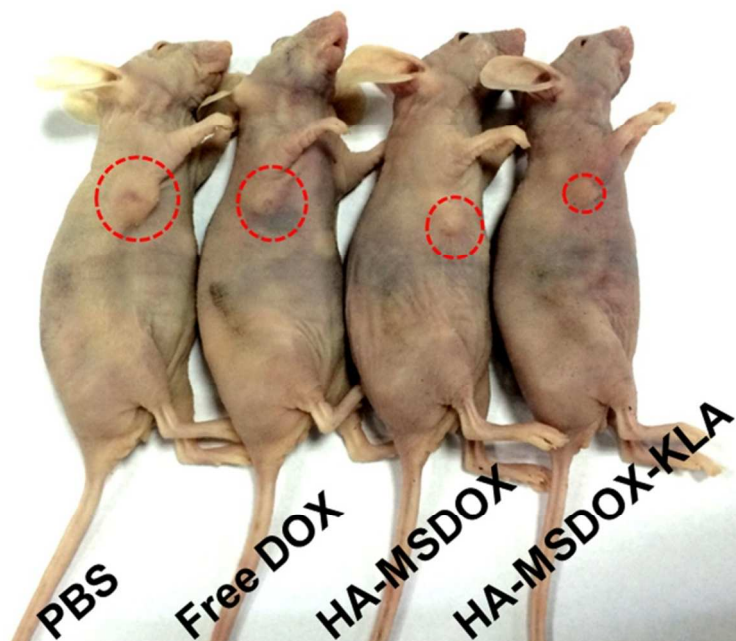


**Figure S16.** Representative images of the MCF-7/ADR xenograft tumors of the mice after treatment with PBS, free DOX, HA-MSDOX, and HA-MSDOX-KLA at day of 16. Red circles indicate the site of tumors.

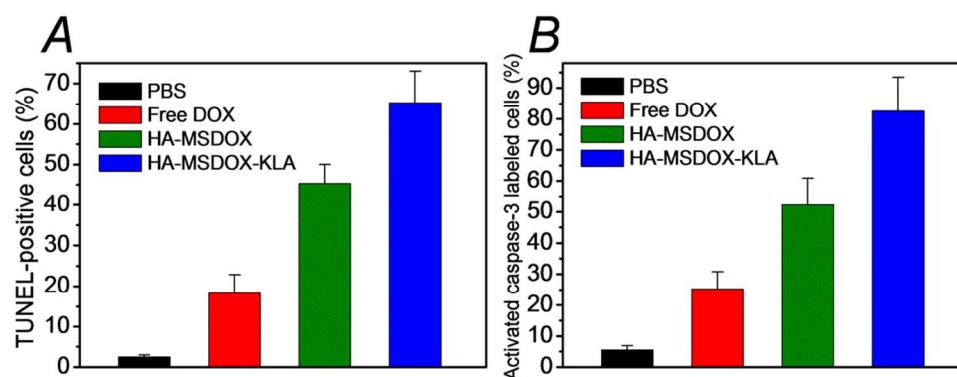


**Figure S17.** A) Quantification of the percentage of TUNEL-positive apoptotic cells in tumors treated with different DOX formulations. B) Quantification of the percentage of activated caspase-3 labeled cells in tumors treated with different DOX formulations.

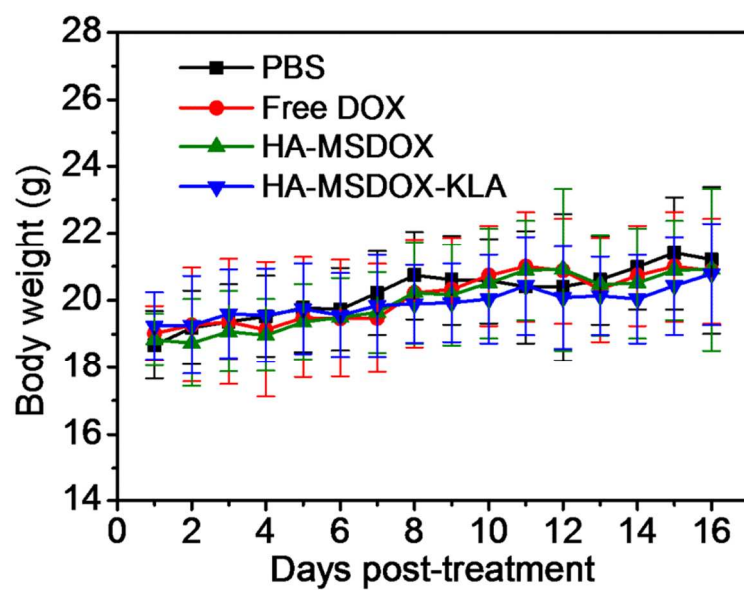


**Figure S18.** The body weight alteration of MCF-7/ADR tumor-bearing mice after different treatments.

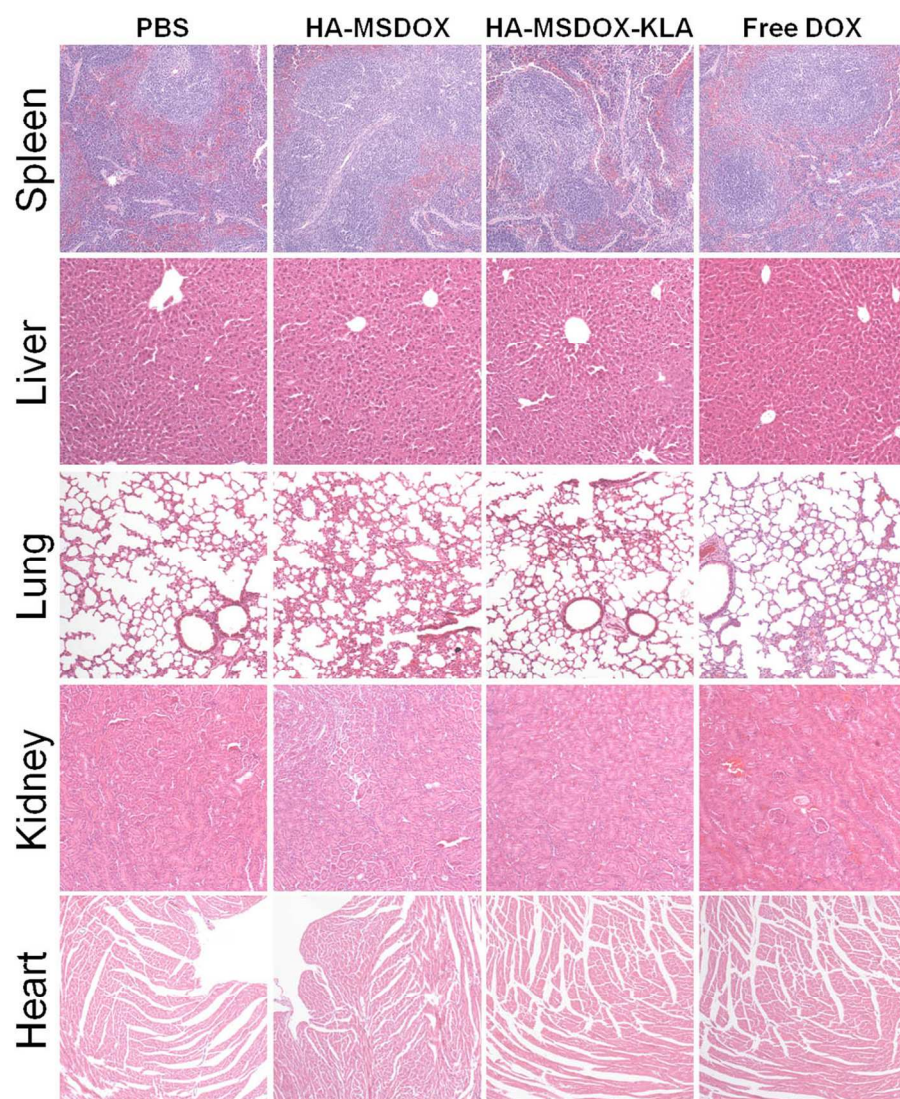


**Figure S19.** Major organs (spleen, liver, lung, kidney, and heart) stained with H&E after different treatments. Compared with PBS control group, no appreciable physiological morphology changes and undetectable adverse effects were observed after HA-MSDOX-KLA treatment, suggesting that almost no damage of HA-MSDOX-KLA to organs in the *in vivo* assessments.